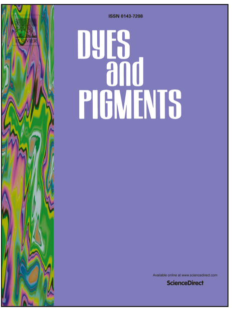

Tetrabenzeneaza Macrocycle: A Novel Platform for Universal High-performance Hole Transport Materials

Jiangnan Zhu, Wenxuan Song, Tianmei Zhang, Qingchen Dong, Jinhai Huang, Haitao Zhou, Jianhua Su

PII: S0143-7208(20)31678-8

DOI: https://doi.org/10.1016/j.dyepig.2020.108981

Reference: DYPI 108981

To appear in: *Dyes and Pigments*

Received Date: 18 August 2020

Revised Date: 29 October 2020

Accepted Date: 30 October 2020

Please cite this article as: Zhu J, Song W, Zhang T, Dong Q, Huang J, Zhou H, Su J, Tetrabenzeneaza Macrocycle: A Novel Platform for Universal High-performance Hole Transport Materials, *Dyes and Pigments*, https://doi.org/10.1016/j.dyepig.2020.108981.

Tetrabenzeneaza Macrocycle: A Novel Platform for Universal High-performance Hole Transport Materials

Statement:

Under the supervision of colleagues, Jiangnan Zhu (the first author) prepared the compounds contained in the article, performed tests, data analysis, performed calculations and wrote. Wenxuan Song (the second author) developed theoretical calculation and analysis. Tianmei Zhang participate in compound preparation. Others reviewed and modified the article. I agreed to be accountable for all aspects of this work in ensuring that questions related to the accuracy or integrity of any part of the work are appropriately investigated and resolved, and I have approved the final version to be published. All authors read and contributed to the manuscript.

Yours sincerely,

Jianhua Su

Graphical Abstract

Tetrabenzeneaza Macrocycle: A Novel Platform for Universal High-performance Hole Transport Materials

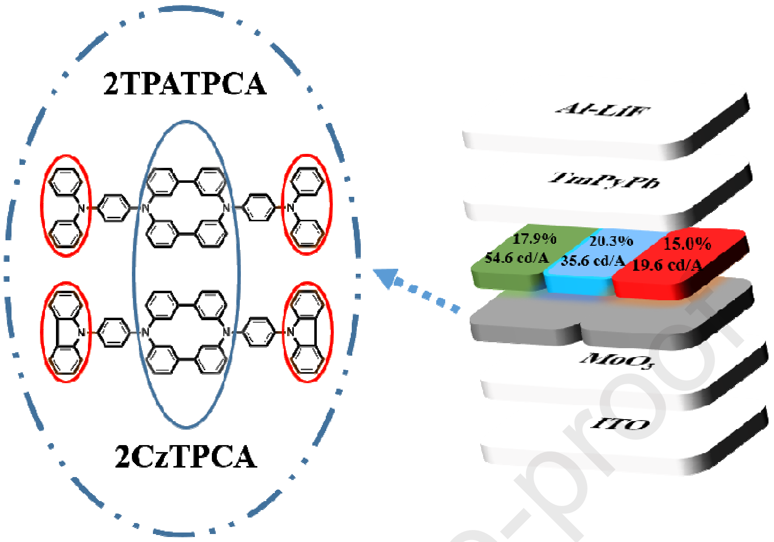

Tetrabenzeneaza Macrocycle: A Novel Platform for Universal High-performance Hole Transport Materials

Jiangnan Zhu[a]. *Wenxuan Song*[a]. *Tianmei Zhang*[a]. *Qingchen Dong*[b]. *Jinhai Huang*[c]. *Haitao Zhou**[a]. *Jianhua Su**[a].

[a]*Key Laboratory for Advanced Materials and Feringa Nobel Prize Scientist Joint Research Center, Institute of Fine Chemicals, School of Chemistry & Molecular Engineering, East China University of Science & Technology, Shanghai 200237, PR China. Fax: (86)21-64252288；Tel: (86)21-64252288；E-mail: bbsjh@ecust.edu.cn*

[b]*MOE Key Laboratory for Interface Science and Engineering in Advanced Materials and Research Center of Advanced Materials Science and Technology, Taiyuan University of Technology, 79 Yingze West Street, Taiyuan 030024, PR China.*

[c]*Zhejiang Baike Semiconductor Material Co. Ltd, Zhejiang, PR China.. E-mail: dele12@163.com*

Abstract

In this research, a novel macrocycle containing tetrabenzeneaza has been developed as a novel building block for hole transport materials (HTMs). Benefiting from its unique highly twisted spatial configuration, this macrocycle exhibits high triplet energy level (E_T) as well as high hole mobility. Based on this aza macrocycle, two hole transporting materials, namely **2TPATPCA** and **2CzTPCA**, were designed and synthesized. Both **2TPATPCA** and **2CzTPCA** possess enough E_Ts, appropriate frontier orbital energy levels as well as good thermal stability, which promote them as universal HTMs in multicolor phosphorescent organic light-emitting devices (PhOLEDs) and thermal activated delay fluorescence (TADF) OLEDs. High external quantum efficiencies (EQEs) were realized in OLEDs using the these two HTMs. For example, sky bule PhOLED with **2CzTPCA** showed a significantly improved maximum EQE of 20.3 % compared to that of the reference device using **N,N'-Bis(naphthalen-1-yl)-N,N'-bis(phenyl)benzidine** (**NPB**) (EQE of 14.2 %) and **4,4'-Cyclohexylidenebis[N,N- bis(4-methyl phenyl)aniline** (**TAPC**) (EQE of 12.2 %) . Green TADF OLED using **2CzTPCA** as HTM also exhibit a much improved maximum EQE of 17.9 % compared to that of the reference device based on **NPB** (EQE of 10.3 %). These results indicate this tetrabenzeneaza macrocyclic is a promising building block for developing universal high-performance HTMs.

Keywords: tetrabenzenacyclohexaphane, universal HTL materials, thermal activated delay fluorescence organic light-emitting diodes, phosphorescent organic light-emitting diodes, high efficiency.

1. Introduction

In the past two decades, OLEDs have attracted considerable attention because of its superb advantages, such as high electroluminescence (EL) efficiency, wider viewing angle, better contrast ratio, lower cost and power comsumption [1-13]. Generally, OLEDs possess sandwich-like multilayer structure which include the anode, hole injection layer (HIL), hole transport layer (HTL), emitting layer (EML), electron transport layer (ETL), electron injection layer (EIL) and the cathode, among which the hole transport layers take the largest material consumption of the devices and have crucial impacts on the devices' EL performance.

Typical HTMs are mainly based on aromatic amines, such as triphenylamine and carbazole, many of which were very successful and achieved excellent EL performance, for instance, **4,4'-Cyclohexylidenebis[N,N- bis(4-methyl phenyl)aniline** (**TAPC**), **N,N'-Bis(naphthalene-2-yl)-N; N, N'-Di-2-naphthyl-N,N'-diphenylbenzidine** (**NPB**) and **N, N'-Bis(naphthalen-1-yl)-N** (**NPD**). However, these HTMs encountered several drawbacks such as poor thermal stability with a low glass transition temperature, which could lead to devices stability and efficiency issues. Therefore, development of new HTMs with superb efficiency and stability is urgently desired.

In this work, a novel building block **tetrabenzenacyclohexaphane** (**TPCA**), which consists of two biphenyl unit connected by two nitrogen atoms, was designed to construct

HTMs for high-performance OLEDs. This bulky and twisted moiety, which possesses excellent thermal stability and appropriate hole transport mobility, provided a new platform to develop HTMs. On that account, two original HTMs, namely **2TPATPCA** and **2CzTPCA**, based on **TPCA** were presented by connecting with the universal building blocks, i.e., triphenylamine and carbazole [14-17].

The thermal stability is crucial to OLEDs' performance, both **2TPATPCA** and **2CzTPCA** exhibit superior thermal stability with decomposition temperature (T_d) above 450 ^oC and glass transition temperature (T_g) above 170 ^oC. In addition, high hole mobility is achieved for both the two HTMs (6.22×10^{-4} $cm^2\,V^{-1}\,s^{-1}$ and 6.99×10^{-5} $cm^2\,V^{-1}\,s^{-1}$) and the high triplet energy level (E_T) of **2TPATPCA** and **2CzTPCA** indicates that they could host multicolor OLEDs [18-22]. Thus, blue PhOLEDs and green TADF OLEDs based on **2TPATPCA** were fabricated and they exhibited satisfactory performance with the EQEs as high as 20.3 % and 17.9 %, CEs of 35.6 and 54.6 cd A^{-1}. This study indicates that **TPCA** is an excellent building block to construct HTMs for high performance OLEDs.

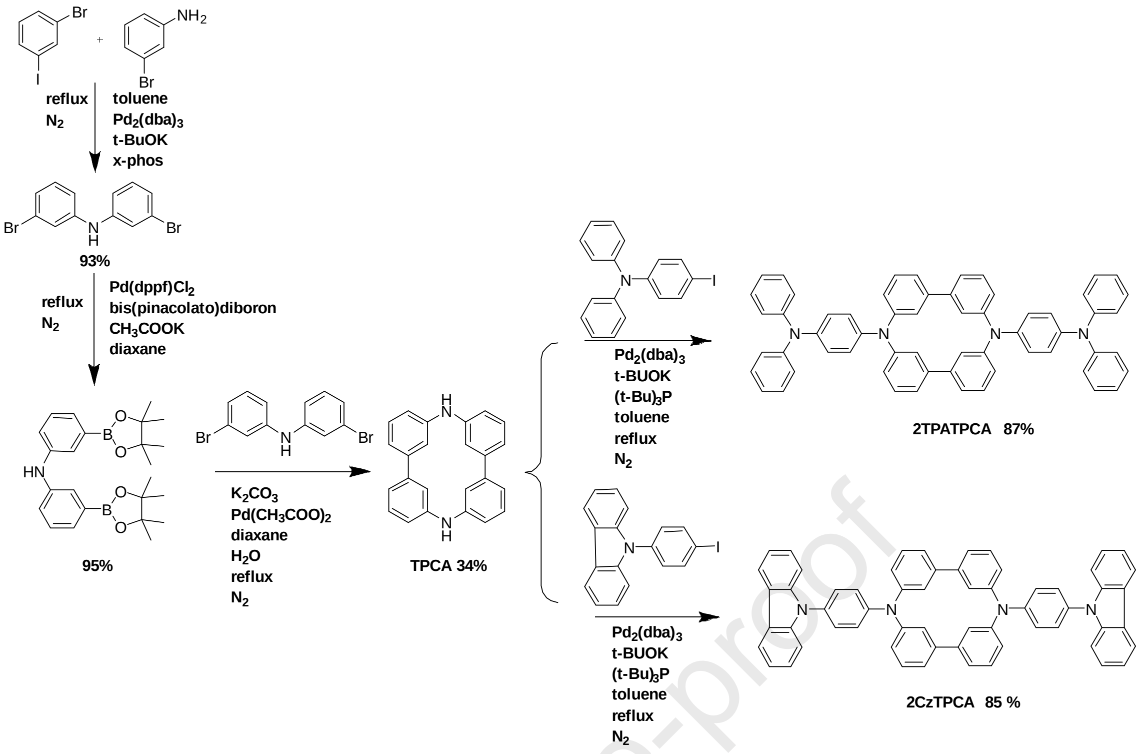

Scheme 1. The synthetic route of **2TPATPCA** and **2CzTPCA**.

2. Experiment

2.1 Synthsis

Synthesis of bis(3-bromophenyl)amine. Add 3-bromoidiobenzene (10 g, 35.4 mmol) and 3-bromoaniline (13.2 g, 42.5 mmol) into a flask, followed by *t*-BuOK (22.3 g, 141.6 mmol), toluene (200 mL) and $Pd_2(dba)_3$ (1.6 g, 1.8 mmol). Heating the mixture to 90 ℃ for 2 h. After completion, dilute aqueous HCl is added, separate the phase and remove toluene, the crude product was purified by silica gel (the eluent composition was DCM:PE=1:20) as a transparent oil (9.3 g, 93 %). ^{1}H NMR (400 MHz, $CDCl_3$) δ: 7.20 (t, J =2.0 Hz, 2H), 7.13(t, J = 8.0 Hz, 2H), 7.10-7.06 (m, 2H), 6.99-6.96 (m, 2H), 5.72 (s, 1H). ^{13}C NMR (101 MHz, $CDCl_3$) δ: 143.8, 130.8, 124.6, 123.2, 120.8, 116.6. HRMS (m/z): Found：$[M–H]^-$ 323.9020，molecular formula $C_{12}H_9Br_2N$ requires $[M–H]^-$ 323.9024.

Synthesis of bis(3-(4,4,5,5-tetramethyl-1,3,2-dioxaborolan-2-yl)phenyl)amine. Add bis(3-bromophenyl)amine (2.0 g, 6.2 mmol), bis(pinacolato)diboron (4.7 g, 15.6 mmol), $Pd(dppf)Cl_2$ (0.5 g, 3.1 mmol) and potassium acetate (3.6 g, 37.4 mmol) into 250 mL flask, followed 100 mL diaxane, reflux the mixture under nitrogen protection for 8 h. The solvent was removed by rotary evaporation, the crude product was purified by silica gel column (the eluent composition was DCM:PE=1:10 to DCM:PE=1:5) as white solid (1.9 g, 95 %).^{1}H NMR (400 MHz, $CDCl_3$) δ: 7.44 (d, J = 2.4 Hz, 2H), 7.38-7.35 (m, 2H), 7.27 (t, J = 7.2 Hz, 2H), 7.24-7.19(m, 2H), 5.69 (s, 1H), 1.60 (s, 24H). ^{13}C NMR (101 MHz, $CDCl_3$) δ: 142.6, 128.7, 127.2, 124.3, 120.3, 83.7, 83.5, 25.0. HRMS(m/z): Found：$[M+Na]^+$ 444.2503，molecular formula $C_{24}H_{33}B_2NO_4$ requires $[M+Na]^+$ 444.2494.

Synthesis of 3,6-diaza-1,2,4,5(1,3)-tetrabenzenacyclohexaphane. Add bis(3-bromophenyl)amine (1.8 g, 5.4 mmol), bis(3-(6,6,7,7-tetramethyl-1,5,3-dioxaborepan-3-yl)phenyl)amine (1.9 g, 4.5 mmol), potassium carbonate (1.9 g, 13.6 mmol) and palladium acetate (50.7 mg, 0.23 mmol) into a 250 mL flask, followed by 120 mL dioxane and 40 mL water, reflux the mixture under nitrogen protection for 8 h. After completion, the solvent was removed and the residue was purified by silica gel column (the eluent composition was EA:PE=1:20 to EA:PE=1:6) to obtain the product as white solid (650 mg, 34%). ^{1}H NMR (400 MHz, DMSO) δ 8.64 (s, 2H), 7.93 (s, 4H), 7.27 (t, J = 8.0 Hz, 4H), 7.00 (d, J = 7.6 Hz, 4H), 6.86 (dd, J = 8.0, 2.0 Hz, 4H). ^{13}C NMR (101 MHz, $CDCl_3$) δ:143.5, 142.3, 129.5, 120.8, 118.2, 116.7. HRMS(m/z): Found：[M+H]$^+$ 333.1389，molecular formula $C_{24}H_{18}N_2$ requires [M+H]$^+$ 333.1392.

Synthesis of 4,4'-(3,6-diaza-1,2,4,5(1,3)-tetrabenzenacyclohexaphane-3,6-diyl)bis(N,N-diphenylaniline). Add 3,6-diaza-1,2,4,5(1,3)-tetrabenzenacyclohexaphane (200 mg, 0.6 mmol) 4-iodo-*N*, *N*-diphenylaniline (267 mg, 0.7 mmol), *t*-BuOK (268 mg, 2.4 mmol) and xylene (100 mL) into Shrek tube, followed by $Pd_2(dba)_3$ (27.5 mg, 0.03 mmol) and $(t\text{-}Bu)_3P$ (0.4 ml), reflux the mixture under nitrogen protection for 4 h. After completion, the solvent was removed under vacuum and the residue was purified by silica gel column (the eluent composition was EA:PE=1:10 to EA:PE=1:3) to get the product as white solid. (174 mg, 87 %).^{1}H NMR (400 MHz, $CDCl_3$) δ: 8.02 (s, 4H), 7.30 (t, *J* = 7.6 Hz, 8H), 7.24 – 7.10 (m, 20H), 7.10 – 6.99(m, 8H), 6.70 (d, *J* = 8.0 Hz, 4H). EA: Found: C 87.6, H 5.3, N 6.8 %; molecular formula $C_{60}H_{44}N_4$ requires C, 87.8; H, 5.4; N, 6.8%. HRMS(m/z): Found：[M+H]$^+$ 821.3631，molecular formula $C_{60}H_{44}N_4$ requires [M+H]$^+$ 821.3644.

Synthesis of 3,6-bis(4-(9H-carbazol-9-yl)phenyl)-3,6-diaza-1,2,4,5(1,3)-tetrabenzenacyclohexaphane. Add 3,6-diaza-1,2,4,5(1,3)-tetrabenzenacyclohexaphane (200 mg, 0.72 mmol), 9-(4-iodophenyl)-9H-carbazole (265 mg, 0.72 mmol), *t*-BuOK (268 mg, 2.4 mmol) and xylene (100mL) into Shrek tube, followed by $Pd_2(dba)_3$ (27.5 mg, 0.03 mmol) and $(t\text{-}Bu)_3P$ (0.4 ml), reflux the mixture under nitrogen protection for 4 h. After completion, the solvent was removed under vacuum and the residue was purified by silica gel column (the eluent composition was

EA:PE=1:10 to EA:PE=1:3) to get the product as white solid. (170 mg, 85 %). ^{1}H NMR (400 MHz, $CDCl_3$) δ: 8.18 (d, J = 7.6 Hz, 4H), 8.03 (s, 4H), 7.68-7.61 (m, 8H), 7.55 (d, J = 8.4 Hz, 4H), 7.51-7.44 (m, 4H), 7.33 (t, J = 7.2 Hz, 4H), 7.27 (t, J = 8.0 Hz, 4H), 7.12 (d, J = 7.6 Hz, 4H), 6.86 (dd, J = 8.0, 2.0 Hz, 4H). EA: Found: C 88.1, H 5.2, N 6.6 %; molecular formula $C_{60}H_{40}N_4$ requires C, 88.2; H, 4.9; N, 6.9%. MS(m/z): Found：$[M+H]^+$ 817.3338，molecular formula $C_{60}H_{40}N_4$ requires $[M+H]^+$ 817.3331.

2.2 Device fabrication and measurement.

Before thermal evaporation at 10^{-4} pa, the **ITO** glass base was washed by acetone, isopropanol and distilled water, all cleaning steps are done in the ultrasound system. Then, the ozone treatment was processed for 10 minutes. All chemical materials were thermally evaporated, at the rate of 0.1 to 3 Å s^{-1}, and the OLEDs devices were measured with a Keithley 2400 source meter and a Minolta CS-2000 spectrometer. All devices characterization were performed at room temperature and in air atmosphere by a record method [23].

3. Results and discussion

3.1 Synthesis and characterization

The synthetic route of **2TPATPCA** and **2CzTPCA** are depicted in Scheme 1. Both the two compounds are synthesized via Buchwald-Hartwig [24-25] and Suzuki Coupling reaction. The structures of **2TPATPCA** and **2CzTPCA** are identified and characterized by ^{1}H and ^{13}C NMR as well as the high-resolution mass spectrometry (HRMS)

Table 1. The physical properties of **2TPATPCA** and **2CzTPCA**.

Molecules	Abs λ_{max}^{a} (nm)	Em λ_{max}^{b} (nm)	E_g^{c} (eV)	E_T^{d} (eV)	HOMO[e] (eV)	LUMO[f] (eV)	T_ds[g] (°C)	T_g^{h} (°C)
2TPATPCA	310	400	3.15	2.76	-5.39	-2.24	440	----
2CzTPCA	301	420	3.30	2.91	-5.39	-2.09	542	179

[a] Measured in **CH_2Cl_2** at a concentration of $1*10^{-5}$ M

[c] Energy gap is calculated by equation E_g=1241/$\lambda_{onset,}$ Onset [26] of the absorption spectra.

[d] Measured in **2-Methyltetrahydrofuran** at 77K

[e] The HOMO energy level was determined from cyclic voltammetry and by E_{HOMO}=4.8+E_{onset}

[f] The LUMO energy is estimated from equation E_{LUMO}=E_{HOMO}+E_g [27-28]

[g] Thermal decomposition temperature was measured by TGA

[h] Glass transition temperature was measured by DSC

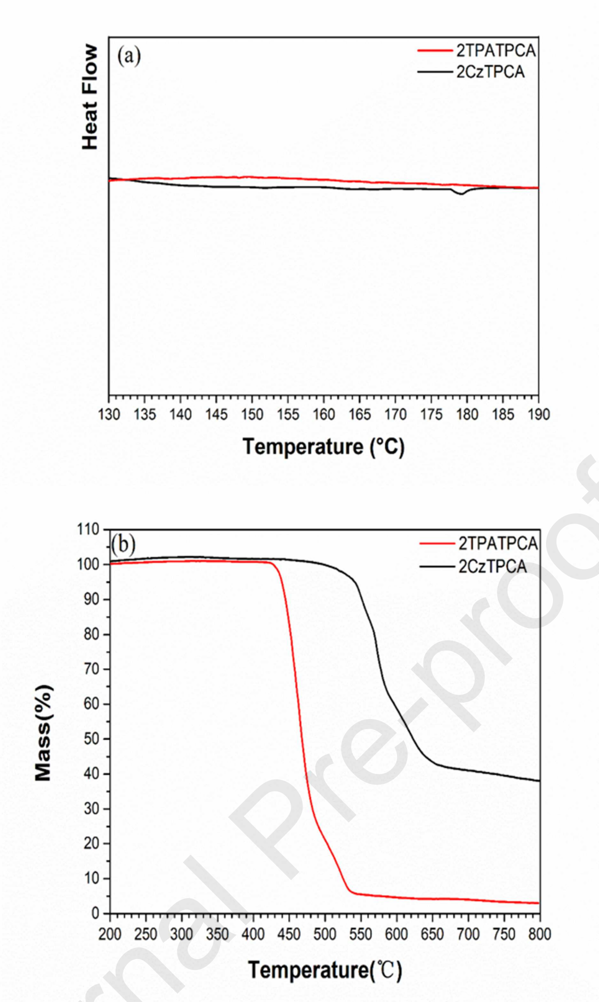

Figure 2. (a) The Differential Scanning Calorimeter analysis of **2TPATPCA** and **2CzTPCA**; (b) The Thermogravimetric Analysis of **2TPATPCA** and **2CzTPCA**.

3.2 Thermal properties

The thermochemical properties of **2TPATPCA** and **2CzTPCA** were investigated by TGA and DSC analysis, and the results are shown in Figure 2 and Table 1. Seen from Figure 2a, **2CzTPCA** exhibits a high T_g of 178 °C, which is much higher than that of **NPB** (95 °C) and TPAC (78 °C). However, the T_g of **2TPATPCA** was not observed. The T_d of **2TPATPCA** and **2CzTPCA** is 430 °C and 550 °C, corresponding to 5% mass loss of compounds, respectively. **2CzTPCA** exhibits higher T_d, which could be ascribed to the more rigid structure of carbazole than triphenylamine. Hence, the TPCA-based compounds possessed excellent thermal stability, which is beneficial to improve the devices' stability and efficiency.

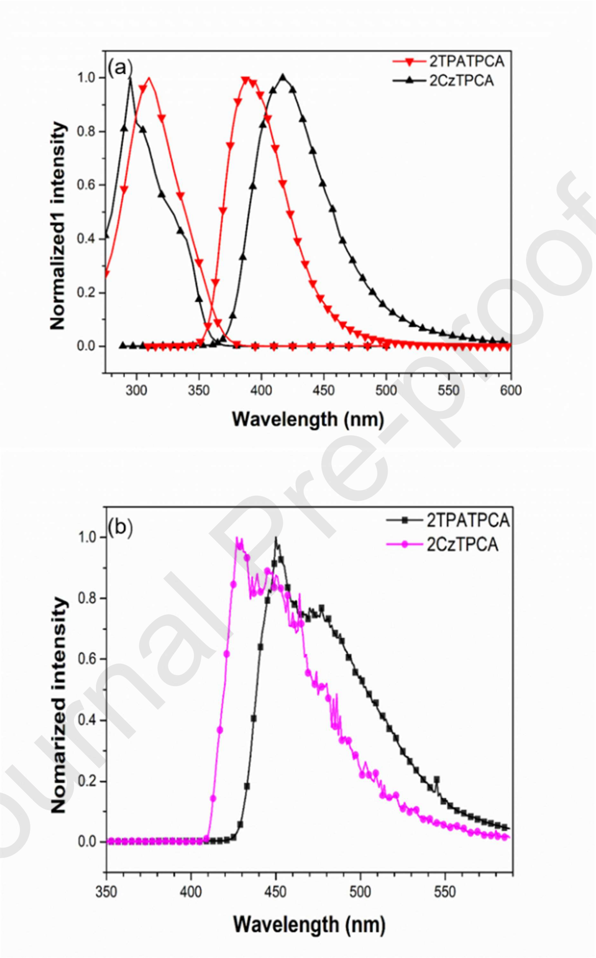

Figure 3. (a) The UV-vis Abs, PL of **2TPATPCA** and **2CzTPCA**; (b) The phosphorescence spectra of **2TPATPCA** and **2CzTPCA**.

3.3 Photophysical properties

As shown in Figure 3 and Table 1, the photophysical properties of the two compounds were similar. The maximum absorption peak of **2TPATPCA** and **2CzTPCA** located at 310 nm and 301 nm, respectively, which could be attributed to the π-π* transition of triphenylamine and 9-phenyl carbazole units. Compared to **2CzTPCA**, the absorption peak of **2TPATPCA** is red-shifted by 9 nm, indicating that **2TPATPCA** possesses a larger extent of charge separation than **2CzTPCA**. Calculated from the onset of absorption peak (λ_{onset}), the energy gap (E_g) of **2TPATPCA** and **2CzTPCA** were determined to be 3.15 and 3.30 eV, while the emission peaks were centered at 400 nm and 420 nm, respectively.

The phosphorescence spectra were recorded in **2-Methyltetrahydrofuran** at 77 K and the triplet energy (E_T) of **2TPATPCA** and **2CzTPCA** were calculated to be 2.76 eV and 2.91 eV, respectively, and the pertinent data were shown in Figure 3b and Table 1. The high E_T qualify **2TPATPCA** and **2CzTPCA** as universal HTMs for multicolor OLEDs.

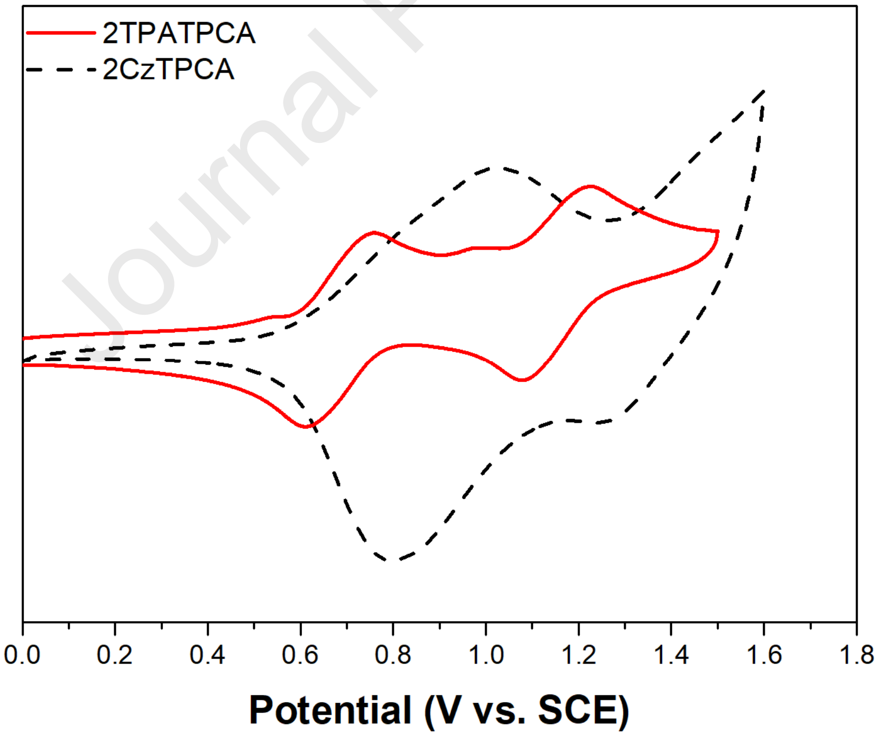

Figure 4. The test result of cyclic voltammetry of **2TPATPCA** and **2CzTPCA** in **CH_2Cl_2** during anodic scans, the two compounds' concentration were $1*10^{-5}$ in **CH_2Cl_2**, the concentration of **Tetrabutylammonium hexafluorophosphate** was 1 mol/L and the Scan rate was o.1V/s.

3.4 Electrochemical properties

Generally, HTMs should have compatible frontier orbital energy levels, i.e., the highest occupied molecular orbital (HOMO) and the lowest unoccupied molecular orbital (LUMO), with the adjacent layers [29]. The HOMO level of a HTM indicates the ease or complexity for holes to pass through the HTL, i.e., from the hole injection layer (HIL) into the emission layer (EML), while the LUMO determines the electron blocking ability, both of them affect the efficiency of OLEDs. The electrochemical properties of **2TPATPCA** and **2CzTPCA** were characterized by cyclic voltammetry (CV) and the pertinent data were shown in the Figure 4 and Table 1. The HOMOs were estimated by the formula $E_{HOMO} = 4.8 + E_{onset}$, while the LUMO was obtained according to the equation: $E_{LUMO} = E_{HOMO} + E_g$. The onset oxidation peaks of **2TPATPCA** and **2CzTPCA** were both located at 0.59 eV, thus the HOMOs were calculated to be -5.39 eV, which is shallower than **NPB** (-5.5 eV) [30] and **TAPC** (-5.6 eV) [31]. The LUMOs of **2TPATPCA** and **2CzTPCA** were decided to be -2.24 eV and -2.09 eV by E_g. The above results revealed that **2TPATPCA** and **2CzTPCA** could be act as potential HTMs.

3.5 Theoretical calculation

The density functional theory was adopted to optimize the ground state geometries of the compounds at the B3LYP/6-31G* level [32] and the pertinent data are depicted in Figure 5. The HOMO of **2TPATPCA** spreads over the whole molecule, while the LUMO mainly locates on the central TPCA moiety, revealing that the compound undergoes a fairly weak separation in the excited state. As to **2CzTPCA**, the HOMO and LUMO is less separated compared to **2TPATPCA**, which might be due to the more planar configuration of carbazole unit than that of triphenylamine.

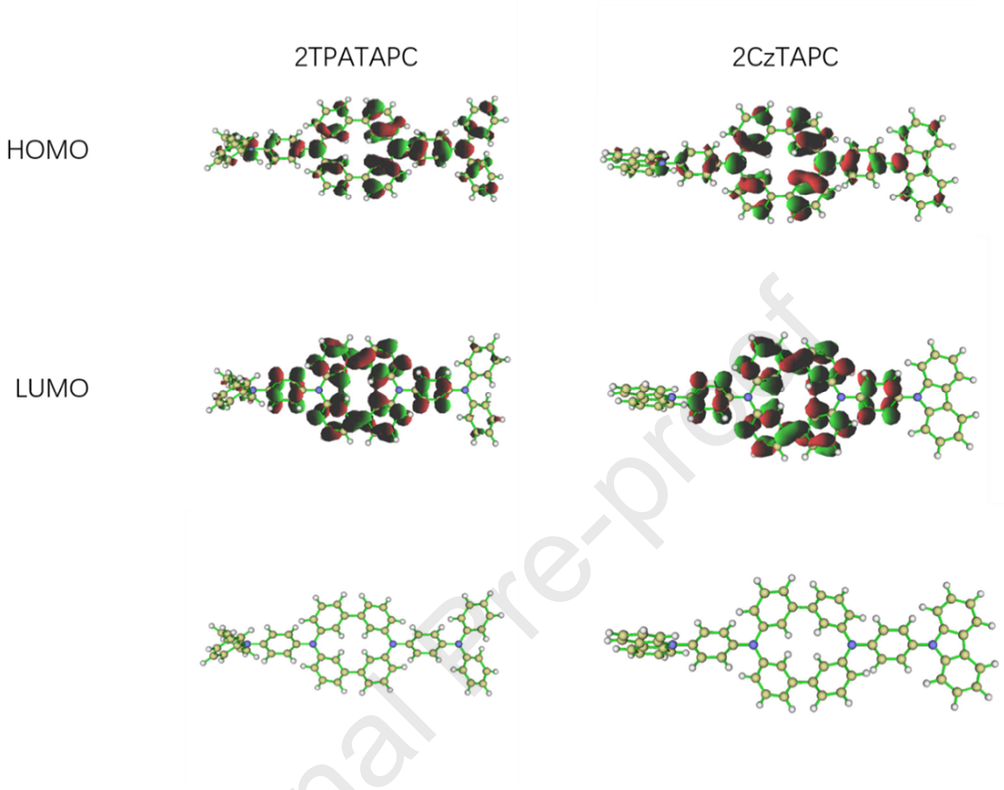

Figure 5. DFT calculation results

3.6 Device structure and characterization

To evaluate the properties of the two HTMs, phosphorescent and TADF OLEDs (red, blue and green) were fabricated. The device structure is **ITO** / **MoO_3** (1 nm) / HTL (40 nm, 60 nm) / EML (emission layer) (20 nm) / **TmPyPB** (55 nm) / **LiF** (0.6 nm) /**Al** (80 nm), which is schematically displayed in Figure 6. The phosphorescent emitters were **FIrpic** (blue), **$Ir(ppy)_3$** (green) and **$Ir(pq)_2acac$** (red), while the TADF emitters were **4CzIPN** (green) and **4CzTPN-Ph** (red). **4,4'-Di(9*H*-carbazol-9-yl)-1,1'-biphenyl** (**CBP**) and **1,3-Bis(carbazol-9-yl)benzene** (**mCP**) were chosen as host materials.

3,3'-[5'-[3-(3-Pyridinyl)phenyl][1,1':3',1''-terphenyl]-3,3''-diyl]bispyridine (**TmPyPb**) was adopted as electron transport layer. The doping ratios of red, green and blue emitters were set at 5 wt % in **CBP**, 8 wt % in **CBP** and 8 wt % in **mCP**. EL depends on the HTM thickness (40 nm and 60 nm) of **2TPATPCA** and **2CzTPCA** was investigated and shown in the Figure S3 and Table S1.

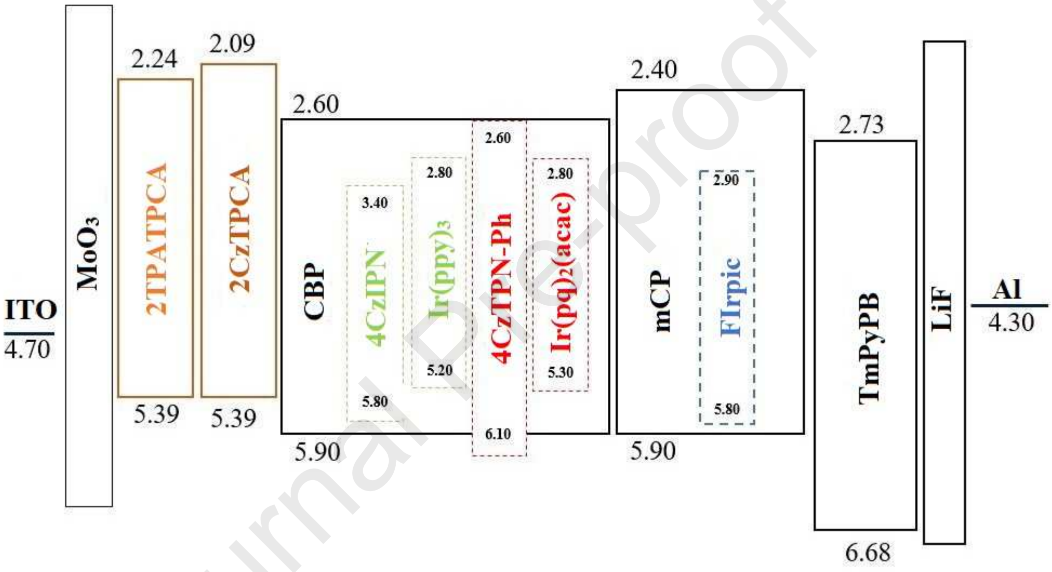

Figure 6. The energy level diagram of the devices002E

3.7 Phosphorescent device (PhOLEDs) characteristics

In order to investigate the electroluminescence performance of **2TPATPCA** and **2CzTPCA**, phosphorescent devices 1 using **2TPATPCA** and devices 2 using **2CzTPCA** were fabricated. The EL performance of PhOLEDs, containing the current-voltage-luminance (J-V-L), external quantum efficiency-luminance (EQE-L), current efficiency-luminance (CE-L) and electroluminescence spectra (EL), are displayed in Figure 7 and Table 2. The power efficiency-luminance curves are shown in Figure S5. The devices are labeled as 1-RP, 1-GP, 1-BP, 2-RP, 2-GP and 2-BP, in which 1 represents for **2TPATPCA**, 2 for **2CzTPCA**, R for red, B for blue, G for green, P for phosphorescent.

Excellent EL performance was achieved from the blue PhOLEDs, for example, the V_{on} and EQE were 3.96 V/ 12.9 % for 1-BP, 3.84 V/ 20.3 % or 2-BP, as shown in Figure 7a and 7b, the CE (Figure 7c) and PE (Figure S5a) were 28.7 cd A^{-1} /16.5 lm W^{-1} for 1-BP, and 35.6 cd A^{-1}/ 25.8 lm W^{-1} for 2-BP. The highest CE and brightness was obtained from the green ones, for 1-GP was 55985 cd m^{-2}/ 24.9 lm W^{-1}, and 2-GP was 27968 cd m^{-2}/ 31.1 lm W^{-1}. It worth noting that the brightness of all the PHOLEDs reached the requirement of commercial applications. However, the performance of those red ones was rather embarrassing for their higher V_{on}, lower CE and PE. Remarkably, all devices possessed low efficiency roll-off, which was only 5 %-10 % in the range of 100 to 1000 cd m^{-2}. Meanwhile, the EL spectra were recorded and the results were shown in Figure 7d and S4. It could be seen that the EL spectra are nearly voltage independent.

By and large, the **2CzTPCA**-based devices showed better EL performance than that of **2TPATPCA**, which could be attributed to the shallower LUMO， besides, **2CzTPCA** has higher E_T, hence possesses better electron blocking ability than **2TPATPCA**. As to the wide difference between the red and blue OLEDs, the lower energy barrier and more matched triplet energy levels of the blue ones might be the principal factors. Compared with the triplet energy of blue and green emitting materials, the red emitting materials have the lowest triplet energy level, and the triplet energy level of **2TPATPCA** is lower than **2CzTPCA**, so **2TPATPCA** performs better than **2CzTPCA** in red devices, but worse in blue ones.

Additionally, those blue PHOLEDs with superior EL performance were selected to compare with the **NPB and TAPC** based devices, as shown in Figure S8 and Table 2, and the results demonstrated that **2TPATPCA** and **2CzTPCA** exhibited better EL performance than the traditional **NPB and TAPC** counterpart, which might be due to their more appropriate energy levels and T_g.

Table 2 The device properties based on different EML

Device	EML	hosts	V_{on}[a] (V)	L[b] (cd m^{-2})	N_c[c] (cd A^{-1})	n_p[d] (lm W^{-1})	n_{ext}[e] (%)	CIE[f] (x,y)
1-BP	**FIrpic**	**mCP**	3.96	13410	28.5/26.4/28.7	16.5	12.7/12.4/12.9	（0.15，0.29）
2-BP	**FIrpic**	**mCP**	3.84	9528	34.9/30.1/35.6	25.8	20.2/17.1/20.3	（0.15，0.29）
NPB	**FIrpic**	**mCP**	4.51	9257	24.7/20.4/25.9	17.4	14.2/11.8/14.6	（0.15，0.29）
TAPC	**FIrpic**	**mCP**	4.72	5338	18.7/18.3/21.2	10.7	11.1/10.5/12.2	（0.15，0.29）
1-GP	**$Ir(ppy)_3$**	**CBP**	3.94	55985	36.8/46.7/47.4	24.9	11.1/13.6/13.8	（0.32，0.61）
2-GP	**$Ir(ppy)_3$**	**CBP**	3.90	27968	41.8/43.1/44.6	31.1	13.0/12.7/13.2	（0.32，0.61）
1-RP	**$Ir(pq)_2(acac)$**	**CBP**	3.59	18814	25.6/22.5/26.6	19.1	14.4/12.3/15.0	（0.62，0.38）
2-RP	**$Ir(pq)_2(acac)$**	**CBP**	4.78	10081	19.5/17.8/19.6	11.8	9.7/7.9/10.5	（0.62，0.38）
1-GT	**4CzIPN**	**CBP**	4.67	13843	48.1/49.0/50.7	26.0	15.5/16.1/16.5	（0.30，0.56）
2-GT	**4CzIPN**	**CBP**	4.36	12098	53.8/48.1/54.6	33.4	17.8/16.1/17.9	（0.30，0.56）
NPB	**4CzIPN**	**CBP**	4.19	9696	31.4/26.4/32.8	21.6	10.3/8.7/10.6	（0.30，0.56）
1-RT	**4CzTPN-ph**	**CBP**	4.83	6998	19.0/16.1/19.6	11.9	8.9/7.5/9.3	（0.56，0.43）
2-RT	**4CzTPN-ph**	**CBP**	5.65	3057	21.3/17.3/23.3	24.1	11.3/10.5/12.5	（0.56，0.43）

[a] Turn-on voltage at luminance was 1cd m^{-2}

[b] The maximum luminance

[c] The current efficiency at the 100 cd A^{-1}, 1000 cd A^{-1}, and the maximum current efficiency，

[d] The maximum power efficiency

[e] The external quantum efficiency at the 100 cd A^{-1}, 1000 cd A^{-1}, and the maximum EQE.

[f] The CIE coordinate at 6 V.

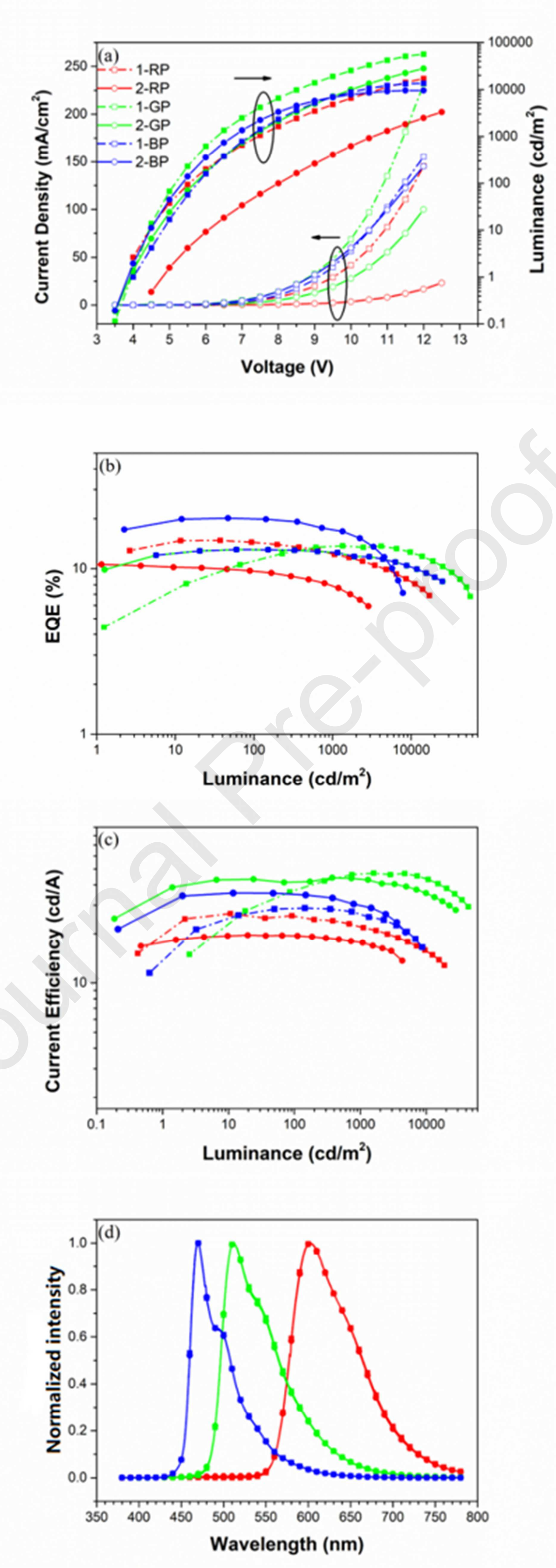
(a)
1-RP
2-RP
1-GP
2-GP
1-BP
2-BP
Current Density (mA/cm²)
Luminance (cd/m²)
Voltage (V)
0
50
100
150
200
250
0.1
1
10
100
1000
10000
100000
3
4
5
6
7
8
9
10
11
12
13
(b)
EQE (%)
Luminance (cd/m²)
1
10
1
10
100
1000
10000
(c)
Current Efficiency (cd/A)
Luminance (cd/m²)
10
0.1
1
10
100
1000
10000
(d)
Normalized intensity
Wavelength (nm)
0.0
0.2
0.4
0.6
0.8
1.0
350
400
450
500
550
600
650
700
750
800

Figure 7. The EL performance of the PhOLEDs. (a) The curve of current-voltage-luminance (J-V-L). (b) The curve of external quantum efficiency-luminance (EQE-L). (c) The relationship of current efficiency-luminance (CE-L). (d) The electroluminescence spectra of PhOLEDs.

3.8 TADF devices characteristics

On account of the excellent performance of PhOLEDs, the TADF OLEDs were investigated, and the results are shown in Figure 8 and Table 2 (1-RT represents for Red-TADF OLED and 1-GT for Green-TADF of **2TPATPCA**, 2-RT and 2-GT of **2CzTPCA**). Seen from the results illustrated in Figure 8a and 8b, excellent performance was obtained from the green OLEDs, for instance, V_{on}/EQE is 4.67 V/ 16.5 % for 1-GT and 4.36 V/ 17.9 % for 2-GT, while the red OLEDs were 4.83 V/9.3 % for 1-RT and 5.65 V/ 12.5 % for 2-RT. Obviously, the **2CzTPCA**-based OLEDs showed better performance than the **2TPATPCA**-based ones, this may be due to **2CzTPCA** has a higher triplet energy and a shallower LUMO, which could prevent the energy transfer from guest to host. The higher efficiency of the green devices than the red ones could be predicted and explained by this as well. Furthermore, all device possessed low efficiency roll-off of within 10 % while the brightness increased from100 to 1000 cd m^{-2} and the voltage dependence of the EL spectra was very limited as shown in Figure S4. When compared with **NPB** based OLEDs, of which EL performance is shown in Figure S7 and Table 2, the **2CzTPCA**-based ones showed distinct advantages. The superb performance of **2TPATPCA** and **2CzTPCA** might be ascribed to their balanced energy levels and high E_T, which could effectively block the reversed transfer of the excitons.

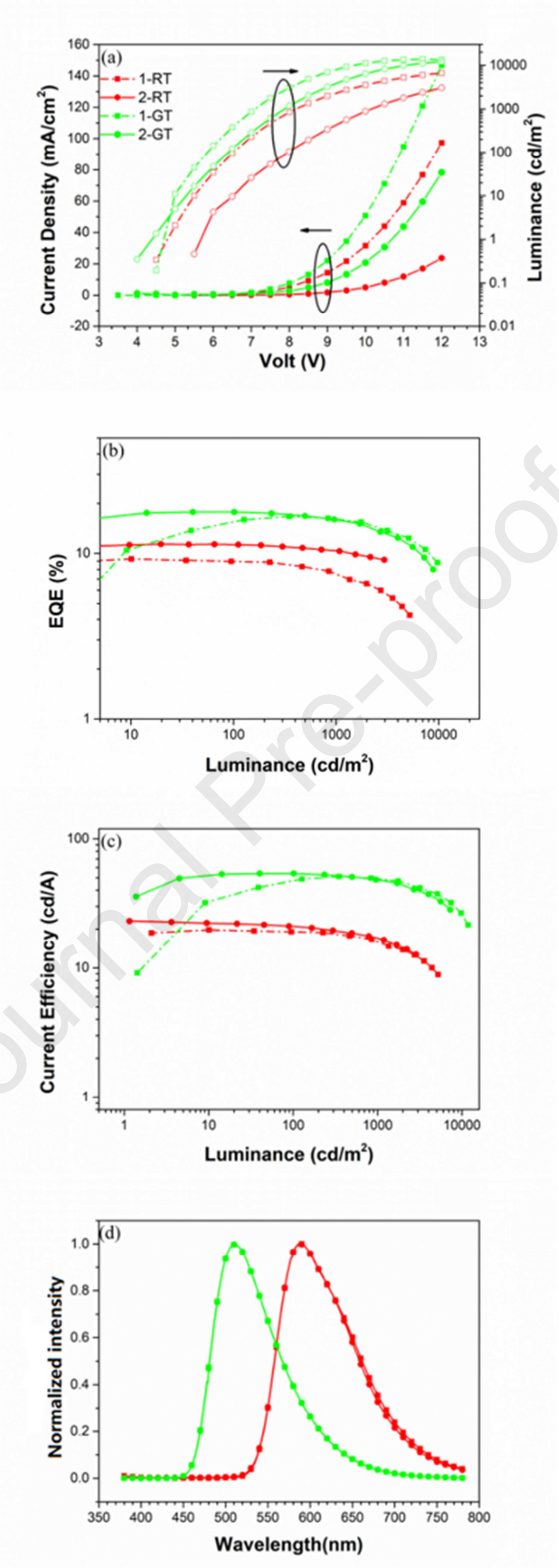
(a)
1-RT
2-RT
1-GT
2-GT
Current Density (mA/cm^2)
Luminance (cd/m^2)
Volt (V)
160
140
120
100
80
60
40
20
0
-20
3
4
5
6
7
8
9
10
11
12
13
10000
1000
100
10
1
0.1
0.01
(b)
EQE (%)
Luminance (cd/m^2)
10
1
10
100
1000
10000
(c)
Current Efficiency (cd/A)
Luminance (cd/m^2)
100
10
1
1
10
100
1000
10000
(d)
Normalized intensity
Wavelength(nm)
1.0
0.8
0.6
0.4
0.2
0.0
350
400
450
500
550
600
650
700
750
800

Figure 8 . The EL performance of the TADF OLEDs. (a) the curve of current-voltage-luminance (J-V-L). (b) The curve of external quantum efficiency-luminance (EQE-L). (c) The relationship of current efficiency-luminance (CE-L). (d) the electroluminescence spectra of TADF OLEDs.

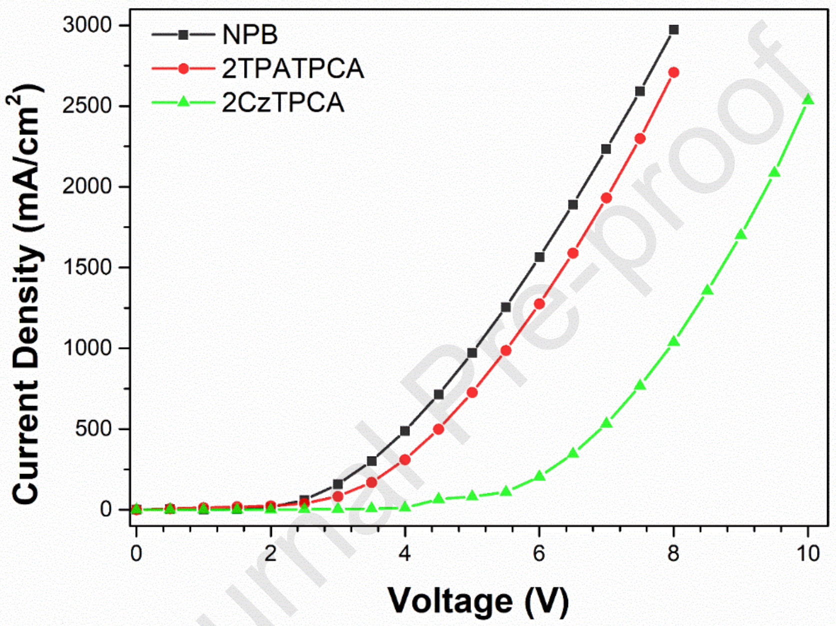

Figure 9. The HOD device performance of the **2TPATPCA**, **2CzTPCA** and **NPB**.

3.9 The hole only device

Hole transport mobility affects the binding rate of holes and electrons, in turn determines the generation of excitons in the EML and indirectly influences the OLEDs' performance. In order to evaluate the hole transport mobility of **2CzTPCA** and **2TPATPCA**, hole only devices (HOD) were fabricated and the two HTMs' hole transport mobilities were calculated by space-charge-limited-current method (SCLC) [33-35]. The device structure was **ITO**/**MoO_3** (1 nm)/HTL (60 nm)/ **MoO_3** (1 nm)/**Al** (80 nm) as shown in Figure 9, and the hole mobility of **2TPATPCA** and **2CzTPCA** were 6.22×10^{-4} and 6.99×10^{-5} $cm^2 V^{-1} s^{-1}$, respectively, utilizing the formula $J= 9\varepsilon_0\varepsilon_r\mu V^2/8L^3$. The hole mobility of **2TPATPCA** is comparable with that of **NPB** (8.32×10^{-4} $cm^2 V^{-1} s^{-1}$), while the counterpart of **2CzTPCA** is about one magnitude smaller than **NPB**.

It could be concluded that the order of EQE of these three HTMs moves opposite their mobility, indicating that higher hole mobility didn't mean better EL performance, since the mobility of hole is one or two magnitude high than that of electron. Therefore, achieving a balanced transport of both holes and electrons in the transport layers is beneficial to elevate the performance OLEDs. The combination of appropriate energy levels, moderate hole mobility and high E_T promoted **2TPATPCA** and **2CzTPCA** as promising candidates for HTMs for high performance OLEDs.

4. Conclusions

In conclusion, two novel HTMs, **2TPATPCA** and **2CzTPCA**, were synthesized and employed in both TADF and phosphorescence RGB OLEDs as HTL. The HOMO/LUMO of **2TPATPCA** and **2CzTPCA** were -5.39 eV/-2.24 eV and -5.39 eV/-2.09 eV, while their E_T were 2.76 eV and 2.91 eV, respectively. Both the two compounds showed outstanding thermal stability. Blue PHOLEDs and the green TADF OLEDs based on **2TPATPCA** and **2CzTPCA** exhibited superior EL performance, which could be attributed to their high E_T and appropriate HOMO/LUMO level. Besides, the **2CzTPCA** based OLEDs exhibited better EL performance than **2TPATPCA**, **NPB** and **TAPC** based ones, for example, **2CzTPCA** based blue PhOLEDs achieved CE of 35.6 cd A^{-1} and EQE of 20.3 %, while the counterpart of **2TPATPCA** was 28.7 cd A^{-1} and 12.9%. For green TADF OLEDs, **2CzTPCA** and **2TPATPCA** incorporated OLEDs revealed CE/EQE of 25.9 cd A^{-1}/ 17.9 % and 50.7 cd A^{-1}/16.5 %. Our study demonstrated that the novel macrocycle containing tetrabenzeneaza could act as a promising building block for designing HTMs for versatile OLEDs.

Acknowledgements

Thanks for the financial support from the NSFC/China (21788102, 21790361), Shanghai Municipal Science and Technology Major Project (Grant No.2018SHZDZX03), the Programme of Introducing Talents of Discipline to Universities (B16017).

References

[1] Tang CW, VanSlyke SA. Organic electroluminescent diodes. Appl Phys Lett. 1987; 51: 913-915.

[2] Zhang Y, Lee J, Forrest SR. Tenfold increase in the lifetime of blue phosphorescent organic light-emitting diodes. Nat Commun 2014; 5: 5008.

[3] Burroughes JH, Bradley DDC, Brown AR, Marks RN, Mackay K, Friend RH, Burns PL, Holmes AB. Light-emitting diodes based on conjugated polymers. Nature 1990; 347: 539-541.

[4] Uoyama H, Goushi K, Shizu K, Nomura H, Adachi C. Highly efficient organic light-emitting diodes from delayed fluorescence. Nature 2012; 492: 234-238.

[5] Gustafsson G, Cao Y, Treacy GM, Klavetter F, Colaneri N. Heeger AJ. Flexible light-emitting diodes made from soluble conducting polymers. Nature 1992; 357: 477-479.

[6] Morkoç H, Strite S, Gao GB, Lin ME, SverdlovB, Burns MB. Large-band-gap SiC, III-V nitride, and II-VI ZnSe-based semiconductor device technologies. J Appl Phys 1994; 76: 1363-1398.

[7] Ai X, Evans EW, Dong S, Gillett AJ, Guo H, Chen Y, Hele TJH, Friend RH, Li F. Efficient radical-based light-emitting diodes with doublet emission. Nature 2018; 563: 536-540.

[8] Han TH, Choi MR, Woo SH, Min SY, Lee CL, Lee TW. Molecularly controlled interfacial layer strategy toward highly efficient simple-structured organic light-emitting diodes. Adv Mater 2012; 24: 1487-93.

[9] Yu D, Zhao F, Zhang Z, Han C, Xu H, Li J, Ma D, Yan P. Insulated donor-pi-acceptor systems based on fluorene-phosphine oxide hybrids for non-doped deep-blue electroluminescent devices. Chem Commun 2012; 48: 6157-6159.

[10] Wang Y, Wang W, Huang Z, Wang H, Zhao J, Yu J, Ma D. High-efficiency red organic light-emitting diodes based on a double-emissive layer with an external quantum efficiency over 30%. J Mate Chem C 2018; 6: 7042-7045.

[11] Sun YR, Giebink NC, Kanno H, Ma BW, Thompson ME, Forrest SR. Management of singlet and triplet excitons for efficient white organic light-emitting devices. Nature 2006; 440: 908-912.

[12] Baldo MA, Thompson ME, Forrest SR. High-efficiency fluorescent organic light-emitting devices using a phosphorescent sensitizer. Nature 2000; 403: 750-753.

[13] Liu Y, Li C, Ren Z, Yan S, Bryce MR. All-organic thermally activated delayed fluorescence materials for organic light-emitting diodes. Nat Rev Mater 2018; 3: 18020.

[14] Xia C, Wang X, Lin J, Jiang W, Ni Y, Huang W. Organic light-emitting devices (OLED) based on new triphenylamine derivatives. Synthetic Met 2009; 159: 194-200.

[15] Adachi C, Tsutsui T, Saito S. Organic electroluminescent device having a hole conductor as an emitting layer. Appl Phy Letter 1989; 55: 1489-1491.

[16] Huang J, Su JH, Tian H. The development of anthracene derivatives for organic light-emitting diodes. J Mater Chem C 2012; 22: 10977-10989.

[17] Aziz H, Popovic ZD, Hu NX, Hor AM, Xu G. Degradation Mechanism of Small Molecule-Based Organic Light-Emitting Devices. Science 1999; 283: 1900-1902.

[18] Zhang D, Song X, Cai M, Duan L. Blocking Energy-Loss Pathways for Ideal Fluorescent Organic Light-Emitting Diodes with Thermally Activated Delayed Fluorescent Sensitizers. Adv Mater 2018; 30: 1705250.

[19] Zhang D, Qiao J, Zhang D, Duan L. Ultrahigh-Efficiency Green PHOLEDs with a Voltage under 3V and a Power Efficiency of Nearly 110 lm W^{-1} at Luminance of 10 000 cd m^{-2}. Adv Mater 2017; 29: 1702847.

[20] Ding L, Dong SC, Jiang ZQ, Chen H, Liao LS. Orthogonal Molecular Structure for Better Host Material in Blue Phosphorescence and Larger OLED White Lighting Panel. Adv Funct Mater 2015; 25: 645-650.

[21] Zhang Y, Liu C, Hang XC, Xue Q, Xie G, Zhang C, Qin T, Sun Z, Chen ZK, Huang W. Phenylquinoline fused cyclic derivatives as electron acceptors of exciplex forming hosts for solution-processable red phosphorescent OLEDs. J Mater Chem C 2018; 6: 8035-8041.

[22] Cai X, Su SJ. Marching Toward Highly Efficient, Pure-Blue, and Stable Thermally Activated Delayed Fluorescent Organic Light-Emitting Diodes. Adv Funct Mater 2018; 28: 1802558.

[23] Forrest SR, Bradley DDC, Thompson ME. Measuring the Efficiency of Organic Light-Emitting Devices. Adv Mater 2003; 15: 1043-1048.

[24] Yamamoto K, Higashibayashi S. Synthesis of Three-Dimensional Butterfly Slit-Cyclobisazaanthracenes and Hydrazinobisanthenes through One-Step Cyclodimerization and Their Properties. Chem Eur J 2016; 22: 663-671.

[25] Hernandez-Perez, AC, Collins SK. A visible-light-mediated synthesis of carbazoles. Angew Chem Int Ed 2013; 52: 12696-12700.

[26] Song W, Chen Y, Xu Q, Mu H, Cao J, Huang J, Su J. [1,2,4]Triazolo[1,5- a]pyridine-Based Host Materials for Green Phosphorescent and Delayed-Fluorescence OLEDs with Low Efficiency Roll-Off. ACS Appl Mater Interfaces 2018; 10: 24689-24698.

[27] Song W, Shi L, Gao L, Hu P, Mu H, Xia Z, Huang J, Su J. [1,2,4]Triazolo[1,5-a]pyridine as Building Blocks for Universal Host Materials for High-Performance Red, Green, Blue and White Phosphorescent Organic Light-Emitting Devices. ACS Appl Mater Interfaces 2018; 10: 5714-5722.

[28] Li J, Zhang T, Liang Y, Yang R. Solution-Processible Carbazole Dendrimers as Host Materials for Highly Efficient Phosphorescent Organic Light-Emitting Diodes. Adv Funct Mater 2013; 23: 619-628.

[29] Moral M, Muccioli L, Son WJ, Olivier Y, Sancho-García JC. Theoretical Rationalization of the Singlet–Triplet Gap in OLEDs Materials: Impact of Charge-Transfer Character. J Chem Theory Comput 2015; 11: 168-177.

[30] Murawski C, Fuchs C, Hofmann S, Leo K, Gather MC. Alternative p-doped hole transport material for low operating voltage and high efficiency organic light-emitting diodes. Appl Phys Lett 2014; 105: 113303.

[31] Liang X, Yan ZP, Han HB, Wu ZG, Zheng YX, Meng H, Zuo JL, Huang W. Peripheral Amplification of Multi-Resonance Induced Thermally Activated Delayed Fluorescence for Highly Efficient OLEDs. Angew Chem Int Ed 2018; 57: 11316-11320.

[32] Asish KD, Swapan KG. Density-functional theory for time-dependent systems. Phys Rev A 1987; 35: 442-444.

[33] Duan Y, Xu X, Yan H, Wu W, Li Z, Peng Q. Pronounced Effects of a Triazine Core on Photovoltaic Performance-Efficient Organic Solar Cells Enabled by a PDI Trimer-Based Small Molecular Acceptor. Adv Mater 2017; 29: 1605115.

[34] Tsai KW, Hung MK, Mao YH, Chen SA. Solution-Processed Thermally Activated Delayed Fluorescent OLED with High EQE as 31% Using High Triplet Energy Crosslinkable Hole Transport Materials. Adv Funct Mater 2019; 29: 1901025.

[35] Sandanayaka ASD, Matsushima T, Bencheikh F, Terakawa S, Potscavage WJ, Qin C, Fujihara T, Goushi K, Ribierre JC, Adachi C. Indication of current-injection lasing from an organic semiconductor. Appl Phys Express 2019; 12: 061010.

Highlight

1. Developed a novel platform – tetrabenzenacyclohexaphane for building HTMs.
2. Tetrabenzenacyclohexaphane derivatives exhibited high triplet energies, good thermal stability, and high hole-transporting abilities.
3. Universal HTMs based on tetrabenzenacyclohexaphane in multicolor PhOLEDs and TADF OLEDs all exhibited the superior performance.

Declaration of interests

☒ The authors declare that they have no known competing financial interests or personal relationships that could have appeared to influence the work reported in this paper.

☐The authors declare the following financial interests/personal relationships which may be considered as potential competing interests: